Inorg. Chem. **2008**, *47*, 10991−10997

Theoretical Investigation of the Uranyl Ion Sorption on the Rutile TiO_2(110) Face

Hadrien Perron,[†] Jérôme Roques,*[,‡] Christophe Domain,[†] Romuald Drot,[‡] Eric Simoni,[‡] and Hubert Catalette[†]

Electricité de France, EDF R&D, Département Matériaux et Mécanique des Composants, les Renardières, Ecuelles, F-77818 Moret-sur-Loing Cedex, France, and, IPN Orsay CNRS-UMR 8608, Université Paris-Sud 11, Bâtiment 100, F-91406 Orsay Cedex, France

Received July 4, 2008

Canister integrity and radionuclide retention is of first importance for assessing the long-term safety of nuclear waste stored in engineered geologic depositories. Uranyl ion sorption on the TiO_2 rutile (110) face is investigated using periodic density functional theory (DFT) calculations. From experimental observations, only two uranyl surface complexes are observed and characterized. When the pH increases (from 1.5 to 4.5), the relative ratios of these two surface complexes are modified. From a crystallographic point of view, three sorption sites can be considered and have been studied with different protonation states of the surface to account for very acidic and low acidic conditions. The two surface complexes experimentally observed were calculated as the most stable ones, while the evolution of their sorption energies agrees with experimental data.

Introduction

Within nuclear waste geological assessment, canister safety and radionuclide retention is of first importance. In this field, the interaction between solute and surfaces, which is mainly governed by sorption and precipitation processes, is a crucial point. Therefore, a detailed knowledge of the mineral−water interface is of fundamental interest since the corresponding chemical and physical processes play a significant role. This paper deals with the study of the interaction between the uranyl ion, UO_2^{2+}, and the rutile TiO_2(110) face using a theoretical approach. Among the radionuclides of interest and under the pH conditions considered, U(VI) can be considered as an oxo-cation model. In addition, the substrate rutile titanium dioxide is an interesting candidate for many reasons. First, it can be easily found as powder or manufactured single crystal face. Then, this material presents a wide domain of stability as a function of the pH. According to Jones et al.,[1] natural rutile TiO_2 powder is composed of three major crystallographic planes: the (110) at 60% and the (101) and the (100) at 20% each. Due to its photocatalytic properties,[2] titanium dioxide has been the subject of several experimental and theoretical studies leading to an accurate knowledge of its chemical and physical properties. Microscopic studies have brought a detailed characterization of some low index faces at the atomic level in terms of defects, relaxation, and reconstruction.[3] The chemistry of these low index faces, particularly the (110) face, also has been extensively investigated as recently summarized by Diebold.[4] On the theoretical side, some of the pure low index faces have also been studied, as well as their interaction with atomic[5] or molecular compounds.[6]

Finally, it is possible to predict the powder retention properties by characterizing individual faces. Moreover, as

* To whom correspondence should be addressed. Tel: +33(0)169156869. Fax: +33(0)169157150. E-mail: roques@ipno.in2p3.fr.
[†] Electricité de France.
[‡] Université Paris-Sud 11.

(1) (a) Jones, P.; Hockey, J. A. *Trans. Faraday Soc.* **1971**, *67*, 2669. (b) Jones, P.; Hockey, J. A. *Trans. Faraday Soc.* **1971**, *67*, 2679.
(2) (a) Onishi, H.; Iwasawa, Y. *Phys. Rev. Lett.* **1996**, *76*, 791. (b) Murray, P. W.; Condon, N. G.; Thornton, G. *Phys. Rev. B* **1995**, *51*, 10989. (c) Williams, C. C.; Ekerdt, J. G.; Jehng, J. M.; Hardcastle, F. D.; Wachs, I. E. *J. Phys. Chem.* **1991**, *95*, 8791.
(3) (a) Charlton, G.; Howes, P. B.; Nicklin, C. L.; Steadman, P.; Taylor, J. S. G.; Muryn, C. A.; Harte, S. P.; Mercer, J.; McGrath, R.; Norman, D.; Turner, T. S.; Thornton, G. *Phys. Rev. Lett.* **1997**, *78*, 495. (b) Lindsay, R.; Wander, A.; Montanari, B.; Thorton, G.; Harrison, N. M. *Phys. Rev. Lett.* **2005**, *94*, 246102.
(4) Diebold, U. *Surf. Sci. Rep.* **2003**, *48*, 53.
(5) (a) Předota, M.; Zhang, Z.; Fenter, P.; Wesolowski, D. J.; Cummings, P. T. *J. Phys. Chem. B* **2004**, *108*, 12061. (b) Wang, Y.; Hwang, G. S. *Surf. Sci.* **2003**, *542*, 72. (c) Lopez, N.; Nørskov, J. K. *Surf. Sci.* **2002**, *515*, 175.
(6) (a) Jug, K.; Nair, N. N.; Bredow, T. *Surf. Sci.* **2005**, *590*, 9. (b) Bandura, A. V.; Sykes, D. G.; Shapovalov, V.; Truong, T. N.; Kubicki, J. D.; Evarestov, R. A. *J. Phys. Chem. B* **2004**, *108*, 7844.

10.1021/ic801246k CCC: $40.75
Published on Web 10/31/2008

demonstrated before,[7] the (110) face (60% of the natural powder) can be used as model of the rutile powder reactivity toward aqueous uranyl ion. Indeed, the U(VI)/rutile TiO_2(110) has already been experimentally studied[7−10] using complementary techniques such as EXAFS,[8] SSHG,[9] AFM, or DRIFT.[7]

The EXAFS data[8] shows that the uranyl ion sorbs upon the TiO_2(110) face with an inner-sphere mechanism leading to a bidentate surface complex with no aggregation phenomenon. Then, the sorption edges on powder and on single-crystal faces[7] show that the sorption rate increases with the pH (from 1.5 to 4.5). The TRLFS measurements[10] have shown that two surface complexes coexist simultaneously with a relative ratio depending on the pH. Unfortunately, this technique does not allow one to draw conclusion about the numbers of sorption sites and on the exact nature of the surface complexes. However, regarding the speciation diagram of the uranium ion[9] and since the experiments were performed in the 1.5−4.5 pH range, the uranyl ion is the major species in solution. These two surface complexes thus correspond to an uranyl ion sorbed upon two different sorption sites. The AFM experiments[7] have shown that the single-crystal face is composed of large terraces (around 100 Å width) of clean surface. This assumption is supported by previous works,[11] which have shown that the exposure of defected TiO_2 surface to liquid water heals defects. Finally, the DRIFT[7] and the SSHG[9] experiments, as well as the modeling of the sorption edges,[9] have allowed characterization of the oxygen surface species involved in the interaction with the uranyl ion. In addition to the geometric parameters given by the EXAFS spectroscopy,[8] the nature of the linked atoms has also been determined.

Each theoretical result of this work was directly compared with experimental data. These combined investigations have been performed with the aim of using the complementarities of the experimental and the theoretical approaches. First, the hydrated uranyl ion has been studied in order to optimize the calculation parameters. Then, in contrast to our previous study[12] the protonation state of the surface was determined by MUSIC and the adsorption of the uranyl ion was investigated as a function of the surface protonation state. An additional study has also been performed on uranyl ion bending in order to make a link between the optimized structures and the EXAFS data.[8]

Theoretical Calculations

Because it was shown in a previous work[12] that the periodic approach is very powerful to model the interaction of uranyl ions with TiO_2(110), in this work, all calculations were performed with the VASP 4.6 code (using periodic density functional theory (DFT) methodology).[13] The generalized gradient approximation (GGA), as defined by Perdew and Wang, for exchange-correlation energy evaluation was used.[14] All atoms were described with pseudopotentials developed on plane wave basis sets generated with the projector augmented wave (PAW) method.[15] Relativistic effects are included in the functional expression as suggested by McDonald.[16] The uranium atom has been described with two different pseudopotentials, a soft one, denoted U_{soft}, with a short cutoff radius and a harder one, denoted U_{hard}, with a larger cutoff radius. Both uranium pseudopotentials described explicitly 14 valence electrons ($6s^2\ 6p^6\ 7s^2\ 5f^3\ 6d^1$), and titanium atoms were then described with four valence electrons ($4s^2\ 3d^2$). Finally, for oxygen atoms, two pseudopotentials (a soft one and a harder one, denoted O_{soft} and O_{hard}, respectively) with the same number of valence electrons ($2s^2\ 2p^4$) were also tested. The oxygen atoms of TiO_2, H_2O, and UO_2^{2+}, are chemically very different and require accurate descriptions. The Brillouin zone was integrated using the Monkhorst−Pack sets of k-points centered at the Γ point with an optimized 450 eV energy cutoff.[17] For a charged unit cell, a neutralizing background charge was assumed by VASP. Atomic positions were relaxed using the conjugate gradient scheme at constant volume with bulk parameters ($a = b = 4.649$ Å, $c = 2.972$ Å) and internal parameter ($x = 0.304$) optimized in a previous paper.[18] The model of the dry rutile TiO_2(110) face, with an elementary area of $(a\sqrt{2})c$ Å^2, has also been previously optimized and then used to investigate the water sorption.[19] This model is composed of a five layer slab with its most internal one frozen to bulk positions in order to mimic the bulk hardness to decrease the size of the surface model needed to reach convergence. In this last study, both molecular and dissociative water sorption mechanisms were investigated on a supercell with a large surface of $(2a\sqrt{2})3c$ Å^2 (six elementary areas). Despite the molecular form being the most stable one for a monolayer coverage, dissociated water molecules can be greatly stabilized with hydrogen bonding. This result is in agreement with experimental data suggesting a coexistence of these two forms.[20] Nevertheless, since the molecular form is found as the most stable one, it has thus been considered here. This surface model gave reliable results and has been used for all the following uranyl ion sorption calculations.

The localized DFT calculations have been performed using the Gaussian 03 code.[21] To make comparisons with the periodic approach results, the PW91 functional was also used. Uranium atoms were described using the Stuttgart small-core effective core potential with $5s^2\ 5p^6\ 6s^2\ 5d^{10}\ 6p^6\ 7s^2\ 5f^3\ 6d^1$ electrons explicitly

(7) Vandenborre, J.; Ph.D. Thesis, University of Paris-Sud, 2005.
(8) Den Auwer, C.; Drot, R.; Simoni, E.; Conradson, S. D.; Gailhanou, M.; Mustre de Leon, J. *New J. Chem.* **2003**, *27*, 648.
(9) Dossot, M.; Crémel, S.; Vandenborre, J.; Grausem, J.; Humbert, B.; Drot, R.; Simoni, E. *Langmuir* **2006**, *22*, 140.
(10) Vandenborre, J.; Drot, R.; Simoni, E. *Inorg. Chem.* **2007**, *46*, 1291.
(11) (a) Pan, J. M.; Maschhof, B. L.; Diebold, U.; Madey, E. *J. Vac. Sci. Technol. A* **1992**, *10*, 2470. (b) Towle, S. N.; Brown, G. E.; Parks, G. A. *J. Colloid Interface Sci.* **1999**, *217*, 299.
(12) Perron, H.; Domain, C.; Roques, J.; Drot, R.; Simoni, E.; Catalette, H. *Radiochim. Acta* **2006**, *94*, 601.
(13) (a) Kresse, G.; Hafner, J. *Phys. Rev. B* **1993**, *47*, 558. (b) Kresse, G.; Hafner, J. *Phys. Rev. B* **1994**, *49*, 14251. (c) Kresse, G.; Furthmüller, J. *Comput. Mater. Sci.* **1996**, *6*, 15. (d) Kresse, G.; Furthmüller, J. *Phys. Rev. B* **1996**, *54*, 11169.
(14) (a) Perdew, J. P.; Wang, Y. *Phys. Rev. B* **1992**, *45*, 13244. (b) Perdew, J. P.; Chevary, J. A.; Vosko, S. H.; Jackson, K. A.; Pederson, M. R.; Singh, D. J.; Fiolhais, C. *Phys. Rev. B* **1992**, *46*, 6671.
(15) (a) Blöch, P. E. *Phys. Rev. B* **1994**, *50*, 17953. (b) Kresse, G.; Joubert, D. *Phys. Rev. B* **1999**, *59*, 1758.
(16) MacDonald, A. H.; Vosko, S. H. *J. Phys. C* **1979**, *12*, 2977.
(17) Monkhorst, H. J.; Pack, D. J. *Phys. Rev. B* **1976**, *13*, 5188.
(18) Perron, H.; Domain, C.; Roques, J.; Drot, R.; Simoni, E.; Catalette, H. *Theor. Chem. Acc.* **2007**, *117*, 565.
(19) Perron, H.; Vandenborre, J.; Domain, C.; Drot, R.; Roques, R.; Simoni, E.; Ehrhardt, J.-J.; Catalette, H. *Surf. Sci.* **2007**, *601*, 518.
(20) Bezrodna, T.; Puchkovska, G.; Shymanovska, V.; Baran, J.; Ratajczak, H. *J. Mol. Struct.* **2004**, *700*, 175.

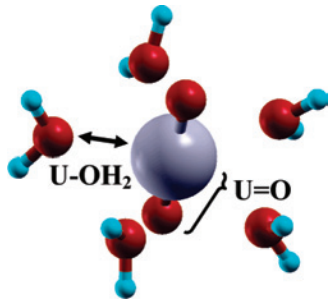

Figure 1. Optimized structure of the pentahydrated uranyl ion, $[UO_2(H_2O)_5]^{2+}$: uranium atom in gray, O atoms in red, and hydrogen ones in blue.

described,[22] while oxygen and hydrogen atoms were described with the 6-31G* all electron basis sets. All calculations were carried out with an "ultrafine" grid for numerical integration, and the Berny algorithm was used for optimization.

Results

Hydrated Uranyl Ion. Uranium is mainly observed in solution in two oxidization states (+IV and +VI) depending on the experimental conditions. The U(VI) is the usual oxidation state observed in aqueous solution under oxic conditions. From the uranium speciation diagram, the uranyl ion is the main species at pH < 4. The localized approach is known to give accurate results on molecular systems, while the periodic one is more appropriate for crystals and surfaces. As a starting point, the efficiency of the periodic approach on molecular systems was studied on the well-known structure of the hydrated uranyl ion, $[UO_2(H_2O)_5]^{2+}$ (see Figure 1). Results after full optimizations are summarized and compared with experimental data and localized calculations in Table 1.

For the periodic approach, all the pseudopotential combinations with U_{soft}, U_{hard}, O_{soft}, and O_{hard} give the same $U-OH_2$ distance and the same O=U=O angle. However, for a given uranium pseudopotential, a shortening of 0.03 Å occurs when the O atom is described by O_{hard} instead of O_{soft}. A similar effect is observed for a given oxygen pseudopotential with a shortening of 0.02 Å between U_{soft} and U_{hard}. The U_{hard}=O_{hard} set is in good agreement with experimental data and localized PW91 or MP2 calculations. Thus, it appeared that the uranyl ion must be described with the two hard pseudopotentials. Nevertheless, there was absolutely no change in the $U-OH_2$ distance whatever the uranium and oxygen pseudopotentials used to describe UO_2^{2+} and H_2O. According to these observations, the oxygen species in water molecules were described with the O_{soft} pseudopotential.

Table 1. Pseudopotential Effects on the Equilibrium Structure of $[UO_2(H_2O)_5]^{2+}$ [a]

	d(U=O)	d(U−OH_2)	θ(O=U=O)
All O_{soft}	1.83/1.81[b]	2.46	179.7
H_2O(hard)/UO_2^{2+}(soft)	1.83/1.81[b]	2.46	179.7
H_2O(soft)/UO_2^{2+}(hard)	1.80/1.78[b]	2.46	179.7
All O_{hard}	1.80/1.78[b]	2.46	179.7
PW91	1.77	2.47	179.9
MP2[c]	1.77	2.46	180
EXAFS[d]	1.77 ± 0.02	2.42 ± 0.02	180

[a] Average distances in Å and angles in degrees. Results from previous theoretical and experimental studies are also reported. [b] For U_{soft} and U_{hard} pseudopotential, respectively; same values for d(U−OH_2) and θ(O=U=O). [c] Reference 23. [d] Reference 8.

Table 2. Optimized Bond Lengths (in Å) and Hydration Energies (in eV) for $[UO_2(H_2O)_n]^{2+}$ Complexes

$n = n_1 + n_2$[a]	0	1	2	3	4	4 + 1	5	4 + 2	5 + 1	6
d(U=O)[b]	1.73	1.74	1.76	1.77	1.78	1.78	1.78	1.78	1.79	1.79
d(U−OH_2)[b,c]		2.27	2.33	2.37	2.39	2.41	2.46	2.42	2.46	2.58
$E^{average}_{hydration}$		3.20	2.79	2.70	2.43	2.16	2.18	1.94	1.99	1.85
$E^{n}_{hydration}$		3.20	2.38	2.52	1.61	1.08	1.20	0.86	1.03	0.18

[a] $n_1 + n_2 = n$, water molecules in the first and second hydration shells. [b] Average bond lengths. [c] Considering only the first hydration sphere.

Then, this set of pseudopotentials was used to determine whether this methodology is able to predict the experimentally observed pentahydrated species. Calculations were thus carried out on $[UO_2(H_2O)_n]^{2+}$ complexes, with n from 0 to 6, with all the water molecules in the first hydration shell of the uranyl ion. For n from 4 to 6, additional structures with water molecules in a second hydration sphere were also tested. These structures are labeled $n_1 + n_2$ (= n) where n_1 and n_2 are the number of water molecules in the first and second hydration spheres, respectively. The n_2 water molecules were introduced in order to maximize the hydrogen bonding with the n_1 ones. In each case, the average hydration energy and the stabilization due to the last introduced water molecule were, respectively, calculated using the two following equations:

$$E^{average}_{hydration} = \frac{E^{isolated}_{uranyl} + nE^{isolated}_{water} - E([UO_2(H_2O)_n]^{2+})}{n} \quad (1)$$

$$E^{n}_{hydration} = E^{isolated}_{water} + E([UO_2(H_2O)_{n-1}]^{2+}) - E([UO_2(H_2O)_n]^{2+}) \quad (2)$$

where for eq 1, $E^{average}_{hydration}$ is the average hydration energy per water molecule, $E([UO_2(H_2O)_n]^{2+})$ is the total energy of the $[UO_2(H_2O)_n]^{2+}$ complex, $E^{isolated}_{uranyl}$ and $E^{isolated}_{water}$ are the reference energies for isolated uranyl ion UO_2^{2+} and water molecule, respectively. Then, from eq 2, $E^{n}_{hydration}$ is the stabilization energy due to the nth water molecule introduced and $E([UO_2(H_2O)_{n-1}]^{2+})$ is the total energy of the $[UO_2(H_2O)_{n-1}]^{2+}$ complex. With these notations, the more the energy is positive, the more the complex is stable. Results are summarized in Table 2.

It can be noticed that the U=O bond length converges quickly with n, while larger effects are observed on the

(21) Frisch, M. J.; Trucks, G. W.; Schlegel, H. B.; Scuseria, G. E.; Robb, M. A.; Cheeseman, J. R.; Montgomery, J. A., Jr.; Vreven, T.; Kudin, K. N.; Burant, J. C.; Millam, J. M.; Iyengar, S. S.; Tomasi, J.; Barone, V.; Mennucci, B.; Cossi, M.; Scalmani, G.; Rega, N.; Petersson, G. A.; Nakatsuji, H.; Hada, M.; Ehara, M.; Toyota, K.; Fukuda, R.; Hasegawa, J.; Ishida, M.; Nakajima, T.; Honda, Y.; Kitao, O.; Nakai, H.; Klene, M.; Li, X.; Knox, J. E.; Hratchian, H. P.; Cross, J. B.; Bakken, V.; Adamo, C.; Jaramillo, J.; Gomperts, R.; Stratmann, R. E.; Yazyev, O.; Austin, A. J.; Cammi, R.; Pomelli, C.; Ochterski, J. W.; Ayala, P. Y.; Morokuma, K.; Voth, G. A.; Salvador, P.; Dannenberg, J. J.; Zakrzewski, V. G.; Dapprich, S.; Daniels, A. D.; Strain, M. C.; Farkas, O.; Malick, D. K.; Rabuck, A. D.; Raghavachari, K.; Foresman, J. B.; Ortiz, J. V.; Cui, Q.; Baboul, A. G.; Clifford, S.; Cioslowski, J.; Stefanov, B. B.; Liu, G.; Liashenko, A.; Piskorz, P.; Komaromi, I.; Martin, R. L.; Fox, D. J.; Keith, T.; Al-Laham, M. A.; Peng, C. Y.; Nanayakkara, A.; Challacombe, M.; Gill, P. M. W.; Johnson, B.; Chen, W.; Wong, M. W.; Gonzalez, C.; Pople, J. A. *Gaussian 03*, Revision C.02, Gaussian, Inc., Wallingford, CT, 2004.
(22) Kuechle, W.; Dolg, M.; Stoll, H.; Preuss, H. *J. Chem. Phys.* **1994**, *100*, 7535.

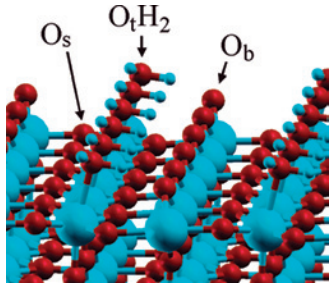

Figure 2. The hydrated rutile $TiO_2(110)$ face: Ti atoms in blue, O ones in red.

U−OH_2 average one. The addition of water molecules in the equatorial plane of the uranyl ion implies a lengthening of the U=O bond of 0.05 Å for $n = 0-5$. The average distances between the uranium atom and the water molecules also increase with n in order to minimize the repulsion between water molecules. Regarding the energies, $E_{\text{hydration}}^{\text{average}}$ and $E_{\text{hydration}}^{n}$ decrease when n increases. The U−OH_2 distances in the first hydration shell are very slightly disturbed by the introduction of the second shell. The average hydration energy does not allow one to distinguish between the relative stabilities of the "4 + 1" and "5" structures (2.16 and 2.18 eV, respectively). For the three structures with $n = 6$ ("4 + 2", "5 + 1", and "6"), the highest average hydration energy is obtained for the "5 + 1" structure. This result is confirmed by the stabilization energy due to this sixth water molecule (1.03 eV versus 0.86 and 0.18 eV for "4 + 2" and "6", respectively). In agreement with experimental data and previous calculations, the pentahydrated uranyl ion, $[UO_2(H_2O)_5]^{2+}$, is characterized as the most stable complex. In addition, the average hydration energy of 2.18 eV calculated for the pentahydrated complex is in agreement with localized PW91 (2.20 eV) and MP2 calculations (2.10−2.17 eV).[23] This good correlation between these results and experimental data, as well as theoretical localized approaches, shows that plane waves periodic DFT calculations can also accurately describe molecular structures such as $[UO_2(H_2O)_5]^{2+}$. This methodology should thus also be able to be used to study the interaction of this species with an oxide surface.

Acid−Base Properties of the Rutile TiO_2(110) Face. In previous studies, periodic dry[18] and hydrated[19] (110) face models have been optimized with the periodic approach. The hydrated rutile $TiO_2(110)$ face (see Figure 2), as defined in ref 19, is composed of a five layers slab with its most internal layer frozen to bulk positions. At the interface, there are three oxygen species: the first one, denoted O_s for surface oxygen, is 3-fold coordinated and is equivalent to a bulk oxygen; the second one, denoted O_b for bridging oxygen, is 2-fold coordinated and is prominent from the surface plane by about 1 Å; finally, the third one, denoted O_t for top oxygen, is single-fold coordinated and arises from the sorption of a water molecule (from the solvent) on a pentacoordinated titanium atom of the dry surface.

For many years, models to predict the acid−base properties at interfaces have been proposed, and the empirical Hiemstra's MUSIC method gives reliable results in many cases.[24] This method is based on the valence Pauling principle stipulating that, in solids, the cation charge is fully compensated by the surrounding oxygen atoms and reciprocally. However, this condition is not any more verified at the surface since some atoms are under-coordinated relative to their bulk environment. This model allows one to evaluate the intrinsic pK values of the different oxygen surface sites by considering their neighborhood and their saturation. By applying this model to the rutile $TiO_2(110)$ face, as it was done in ref 24, we revealed the behavior of the three oxygen surface species: the O_s atom is not reactive to protonation; the O_b atom can be protonated once with a corresponding calculated pK_1 of 4.4; finally the O_t atom is protonated at least once in aqueous solution, and a second protonation is possible with a calculated pK_2 value of 7.5. The third protonation is not possible in aqueous solution. Therefore, starting at very low pH conditions, all O_t atoms are doubly protonated and O_b ones only singly, which corresponds to a saturated surface.

According to the two calculated pK values, when the pH increases, the O_b atoms are first deprotonated, while O_t ones should keep a double protonation state. At pH = pK_1, half of the O_b atoms remain protonated, and the O_t ones are still doubly protonated. Since the difference between the two calculated pK's is large (3.1 logarithmic units), it can be considered that the two corresponding equilibria are well separated.

Uranyl Sorption at Different Surface Protonation States. Since theoretical results from periodic DFT calculations for the isolated aqueous uranyl ion and the hydrated rutile $TiO_2(110)$ face[19] are in good agreement with experimental data, the interaction between both can be investigated using this methodology.

From a crystallographic point of view, three bidentate sorption sites can be envisaged on the hydrated rutile $TiO_2(110)$ face: a bridging−bridging site, denoted *bb*, where the uranyl ion is linked to two O_b atoms of the surface (see Figure 3a); a bridging−top site, denoted *bt*, where the uranyl is linked to one bridging and one top oxygen atom (see Figure 3b); and finally, a top−top site, denoted *tt*, where the uranyl ion is linked to two O_t oxygen atoms (see Figure 3c). To keep its pentadentate equatorial coordination shell, the uranyl ion was saturated with three water molecules. On this $(2a\sqrt{2})3c$ Å^2 surface, the uranyl ion should not interact with its own image since the minimal distance between two uranium atoms is $d(U-U)_{\min} \approx 9$ Å. The uranyl ion can thus be considered as isolated, which is in agreement with EXAFS data where no U−U interaction has been detected.[8]

The protonation states of the different oxygen species, as previously determined by the MUSIC model, were used as

(23) (a) Ismail, N.; Heully, J.-L.; Saue, T.; Daudey, J.-P.; Marsden, C. J. *Chem. Phys. Lett.* **1999**, *300*, 296. (b) Clavaguéra-Sarrio, C.; Ismail, N.; Marsden, C. J.; Bégué, D.; Pouchan, C. *Chem. Phys.* **2004**, *301*, 1. (c) Clavaguéra-Sarrio, C.; Brenner, V.; Hoyau, S.; Marsden, C. J.; Millié, P.; Dognon, J.-P. *J. Phys. Chem. B* **2003**, *107*, 3051.

(24) (a) Hiemstra, H.; Van Riemsdijk, W. H. *J. Colloid Interface Sci.* **1996**, *179*, 488. (b) Hiemstra, T.; Venema, P.; Van Riemsdijk, W. H. *J. Colloid Interface Sci.* **1996**, *184*, 680.

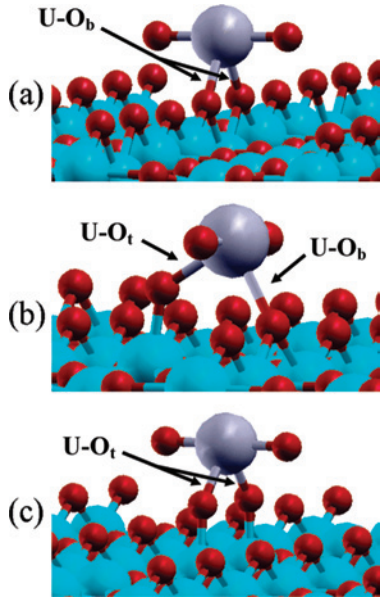

Figure 3. The three crystallographic possible bidentate sorption sites for the uranyl ion on the rutile TiO_2(110) face: (a) *bb* site; (b) *bt* site; (c) *tt* site. Water molecules and hydrogen atoms are not represented to simplify the view.

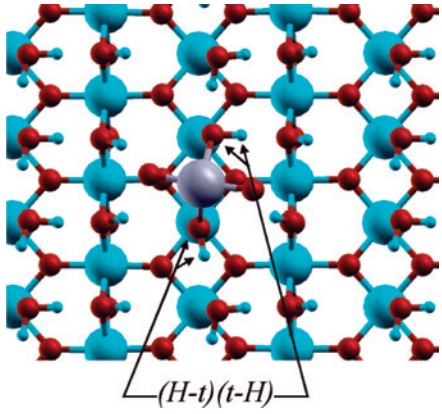

Figure 4. Top view of the *(H-t)(t-H)* structure with the two O_t linked to the uranyl ion singly protonated (water molecules of the uranyl ion hydration sphere have been removed for clarity).

the starting point for the DFT calculations. The first calculations were performed with the uranyl ion directly sorbed as presented in Figure 3 on a saturated surface without removing any protons on O_b or O_t. None of these structures have converged. Thus, for initially protonated O_b atoms, the interaction with the uranyl ion cannot occur if the proton remains linked to the O_b. In the same way, the sorption is not possible on doubly protonated O_t atoms, which should thus be deprotonated at least once. However, all the structures with an uranyl ion linked to one or two O_t−H groups were characterized as energetically favorable and were thus considered. Regarding the three sorption sites represented in Figure 3, six structures can thus be envisaged: three without any hydrogen atoms on the oxygen ones linked to the uranyl ion, denoted *bb*, *bt*, and *tt*; two others with one O_t−H group, *b(t-H)* and *t(t-H)*; one with two O_t−H groups, denoted *(H-t)(t-H)*, which is represented in Figure 4.

These six structures were optimized for surface protonation states that reflect low pH conditions. Such a modeling has already been used in the literature on α-Al_2O_3[25] and TiO_2[26] surfaces and gave reliable results. Experimentally, at low pH conditions, only two surface complexes have been detected: the *bb* site was found as the most stable one, followed by the *bt* one.[7] These six optimized structures were compared with experimental data, and the relative sorption energies of the corresponding surface complexes were calculated (see Table 3).

Table 3. Optimized Geometrical Parameters for the Three Sorption Sites on the Hydrogen-Saturated and Less Protonated Surfaces (Distances in Å, Angles in deg) and Relative Energies (in meV)

	d(U═O)[a]	θ(O═U═O)	d(U−$O_{surface}$)[a]	d(U−O_{water})[a]	$E_{relative}$[b]
			Saturated		
bb	1.91	166.1	2.30	2.60	0.0
bt	1.90	172.3	2.21/2.28[c]	2.62	−85
b(t-H)	1.90	171.6	2.20/2.43[c]	2.62	−274
tt	1.86	176.1	2.17	2.64	−175
t(t-H)	1.86	174.7	2.26	2.66	−190
(H-t)(t-H)	1.85	176.5	2.29	2.67	−417
EXAFS[d]	1.78 ± 0.02	180	2.31± 0.02	2.46 ± 0.02	
			Less Protonated		
bb	1.90	166.1	2.22	2.62	+795
bt	1.86	168.9	2.22/2.24[c]	2.62	+903

[a] Average bond lengths. [b] The *bb* structure on the saturated surface is the most stable one and is taken as reference energy. [c] For O_b and O_t, respectively. [d] Reference 8.

Regarding the sorption energies of these six surface complexes, the *bt* structure was calculated to be nearly 189 meV more stable than the *b(t-H)* one. A similar behavior was observed between the *tt* and the *(H-t)(t-H)* complexes, while only 15 meV separate the *tt* and the *t(t-H)* complexes. In all these cases, the protonated structures were always less stable than their corresponding unprotonated ones. But the most important fact here is that the relative calculated sorption energies agree with the experimental data: the most stable structure at low pH is the *bb* one; the *bt* structure is about 85 meV less stable in agreement with its minor contribution experimentally observed; finally, the *tt* structure is about 175 meV less stable than the *bb* one and should be thus too unstable to be observed, as are the three structures with O_t−H groups. Looking at the U═O and U−O_{water} distances, a part of the lengthening is probably due to the GGA formalism. However, since GGA is also known to give more reliable energies for molecular species than LDA, it has thus been preferently used here. A strong part of this lengthening can also be linked to the lack of the solvent effects, not taken into account in these calculations, which should favor the stabilization of the ═O and −OH_2 bonds. Regarding the U−$O_{surface}$ bond lengths, the average distances determined by EXAFS at 2.31 Å are consistent with almost all the average distances optimized. A lengthening of the U−O_t bond is observed between the *bt* and the *b(t-H)* structures (2.28 and 2.43 Å, respectively), which is certainly due to the added valence on the O_t atom. The same effect was observed for the *tt* structure and its corresponding protonated forms with an increase from 2.17 to 2.29 Å for the U−O_t average bond lengths with the addition of hydrogen

(25) Moskaleva, L. V.; Nasluzov, V. A.; Rösch, N. *Langmuir* **2006**, *22*, 2141.
(26) (a) Barnard, A. S.; Zapol, P.; Curtiss, L. A. *Surf. Sci.* **2005**, *582*, 173. (b) Barnard, A. S.; Zapol, P. *Phys. Rev. B* **2004**, *70*, 235403.

atoms on O_t's. Following these results, the protonation states of all the surface oxygen species are now well-defined: O_b and O_t atoms are, respectively, singly and doubly protonated without uranyl, while they are fully unprotonated when they are linked to the uranyl ion. The three possible bidentate sorption sites described in Figure 3 lead to only two experimentally observed uranyl ion surface complexes on the rutile TiO_2(110) face: *bb* and *bt*. It can also be noticed that the sorbed uranyl ion is not linear in contrast with the pentahydrated form in solution. This bending has already been observed in previous studies on α-Al_2O_3(0001)[25] and $Al(OH)_3$ surfaces.[27] Experimentally, the sorbed uranyl ion is found to be linear, and the observed bending was related to the low bending frequency calculated by Clavaguéra-Sarrio et al. between 100 and 180 cm^{-1} (depending on the exchange−correlation functional used).[23]

Since the two surface complexes detected at low pH with TRLFS are the same as those detected at higher pH, calculations on all the species detailed previously did not need to be performed. Thus, only the two most stable structures (*bb* and *bt*) have been studied for a less protonated surface. The uranyl ion was sorbed on a surface where all the O_b atoms were initially unprotonated but O_t ones were still doubly protonated (see the end of Table 3). No significant effects can be observed on the optimized structures relative to those obtained on the saturated surface. The major difference comes from the sorption energies. Experimentally, the sorption edges show that the amount of sorbed uranyl increases with the pH as expected for a cation because the surface is less and less positively charged. This effect can also indirectly be observed on the different $U-O_{surface}$ bond lengths, which were slightly shorter. In addition, the TRLFS measurements revealed that the relative proportion of the two surface complexes (*bb* and *bt*) is modified when the pH increases.[10] The relative sorption energies have been calculated using as reference energy the *bb* structure on the proton-saturated surface in order to analyze their evolution with decreasing surface protonation (see Table 3). These energies were more stable by around 800 meV, in agreement with the fact that sorption increases with pH. The higher the sorption energies, the greater the sorption rate. This increase in sorption energy is correlated to a shortening of the $U-O_{surface}$ distances, which favors a more important overlap between respective orbitals of the uranium and the surface oxygen atoms. Note that the *bb* complex, which was characterized as the most stable structure on the saturated surface, becomes 108 meV less stable than the *bt* one when the surface is less protonated. Unfortunately, there is no experimental evidence of this stability inversion between the *bb* and the *bt* surface species. However, this phenomenon can be explained by the p*K* values of the different oxygen surface species calculated with the MUSIC model. Starting at low pH, the first oxygen atoms able to be deprotonated are the O_b ones; the *bb* site should thus be favored. As the pH increases, the first deprotonation of the O_t atoms is less and less unfavorable leading to an increase of the *bt* sites.

(27) Veilly, E.; Roques, J.; Jodin-Caumon, M.-C.; Humbert, B.; Drot, R.; Simoni, E. *J. Chem. Phys.*, submitted for publication.

Table 4. Optimized Geometrical Parameters and Relative Energies (in meV) of the Uranyl Ion (Aqueous and Sorbed) as a Function of the O=U=O Angle (Distances in Å, Angles in deg)

θ(O=U=O)	d(U=O)[a]	d(U−OH_2)[a]	$E_{relative}$
	Vacuum		
180	1.78	2.46	0.0
170	1.78	2.47	−41
160	1.79	2.48	−178
150	1.79	2.49	−409
	Sorbed		
166	1.91	2.60	0.0
172	1.91	2.60	−27
177	1.90	2.60	−138

[a] Average bond lengths.

Nevertheless, this last deprotonation should be a really isolated phenomenon, which could explain the fact that the *tt* structure is not observed. Finally, as already observed, the sorbed uranyl ion is bent. In order to clarify this phenomenon, additional calculations have been performed.

Uranyl Bending. In aqueous solution, the pentahydrated uranyl ion is known to adopt a linear structure. Calculations are consistent with this observation (Table 4). In contrast, calculations indicate that the uranyl ion bends spontaneously when it sorbs upon a surface. In order to evaluate the stabilization in energy due to this bending on the surface, some calculations were performed on the most stable *bb* structure in very acidic conditions with different O=U=O angles. For the fully relaxed structure, this angle value is around 166° (see Table 3). Two additional calculations were thus performed with uranyl ions constrained at 172° and 177° with all the other geometrical parameters able to relax (see relative energy variations in Table 4). As expected, the bending effect is at the opposite: the more linear the uranyl ion, the higher the destabilization energy. Nevertheless, these energies are lower that the absolute sorption energies of the uranyl ion and thus should not have significant effects on the whole sorption process.

In addition, a XANES spectrum calculation has shown that until a torsion angle of 20° is reached, the characteristic signal of the uranyl ion (the resonant feature at 50 eV above the white line) is still present.[28] Therefore, taking into account this calculation from the experimental XANES spectrum, the O=U=O angle could be in the range of 160−200°. The calculated structures correspond to energy minima around which the uranyl ion oscillates.

Conclusion

The sorption of the uranyl ion onto the rutile TiO_2(110) face has been investigated using periodic DFT calculations. In the first part, an accurate model of the solvated uranyl ion has been optimized, and the geometrical parameters, as well as the short-range solvation structure, are in agreement with experimental data. In a second part, the sorption of the uranyl ion on the (110) face has been performed at simulated strong and low-acid conditions. These different conditions were simulated by modifying the initial protonation state of the surface oxygen species following the behaviors suggested

(28) Simoni, E.; Den Auwer, C. Personal communication.

by the Hiemstra's MUSIC empirical model. For very acidic conditions, two surface complexes are experimentally observed and have been attributed to the bridging−bridging site (*bb*) and to the bridging−top site (*bt*). On the hydrogen-saturated surface, the *bb* complex was calculated as the most stable one, followed by the *bt* one, which is around 85 meV less stable. The results of the simulations agree with these attributions and show that the third surface complex, the top−top one (*tt*), is certainly too unfavorable to be observed, as are all the structures with O_t still protonated when linked to the uranyl ion. Then, these two most stable surface complexes were studied on a less protonated surface in order to investigate the effects of the protonation state. In agreement with experimental data, the sorbed amount of uranyl ion increases while the two structures evolved differently: initially characterized as the most stable one under strongly acidic conditions, the *bb* structure becomes less stable than the *bt* one. In this paper, both theoretical and experimental results have been directly confronted and correlated with a great coherence on several points. These combined studies show the importance and the complementarities of theoretical and experimental approaches.

Acknowledgment. The CCRT supercomputers within the framework of an EDF-CEA contract and ANR-05-BLAN-0245-03 are gratefully acknowledged.

IC801246K